Electronic Supplementary Information

The direct single- and double-side triol-functionalization of the mixed type Anderson polyoxotungstate $[Cr(OH)_3W_6O_{21}]^{6-}$

Nadiia I. Gumerova,[†] Tania Caldera Fraile, [†] Alexander Roller,[‡] Gerald Giester[§], Magda Pascual-Borràs,[¶] C. André Ohlin[¶] and Annette Rompel*[†]

[†] Universität Wien, Fakultät für Chemie, Institut für Biophysikalische Chemie, Wien, Austria. www.bpc.univie.ac.at

[‡] Universität Wien, Fakultät für Chemie, Zentrum für Röntgenstrukturanalyse, Wien, Austria

[§] Universität Wien, Fakultät für Geowissenschaften, Geographie und Astronomie, Institut für Mineralogie und Kristallographie, Wien, Austria

[¶] Department of Chemistry, Umeå University, Umeå, Sweden. http://www.moleculargeo.chem.umu.se

* Email: annette.rompel@univie.ac.at

1. IR spectroscopy

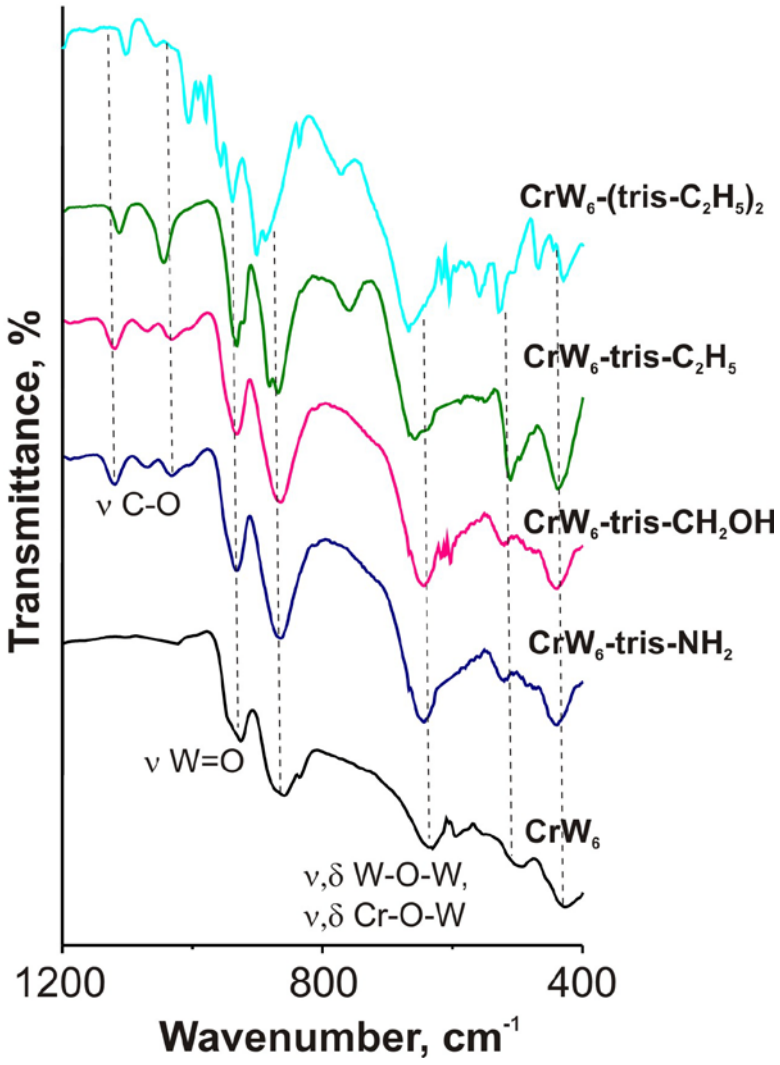

Figure S1. IR spectra of compounds Na_3**CrW_6-(tris-C_2H_5)$_2$**$\cdot 13H_2O$, Na_3K_3**CrW_6-tris-C_2H_5**$\cdot 17H_2O$, Na_5**CrW_6-tris-NH_3**$\cdot 17H_2O$ $Na_4(TMA)_2$**CrW_6-tris-CH_2OH**$\cdot 19H_2O$ and $Na_6[Cr(OH)_3W_6O_{21}]\cdot 22H_2O$.

Table S1. The assignment of IR bands recorded from Na_3CrW_6-(tris-C_2H_5)$_2\cdot 13H_2O$ (= **CrW_6-(tris-C_2H_5)$_2$**), $Na_3K_3CrW_6$-tris-$C_2H_5\cdot 17H_2O$ (= **CrW_6-tris-C_2H_5**), Na_5CrW_6-tris-$NH_3\cdot 17H_2O$ (= **CrW_6-tris-NH_2**), $Na_4(TMA)_2CrW_6$-tris-$CH_2OH\cdot 19H_2O$ (= **CrW_6-tris-CH_2OH**) and $Na_6[Cr(OH)_3W_6O_{21}]\cdot 22H_2O$ (= CrW_6).

	The bands (cm^{-1}) in IR spectra of				
	CrW_6-(tris-C_2H_5)$_2$	**CrW_6-tris-C_2H_5**	**CrW_6-tris-NH_2**	**CrW_6-tris-CH_2OH**	**CrW_6**
δ Cr–O–W	428	435	439	438	430
ν, δ W–O–W	527	513	521	522	520
	668	659	644	646	640
	835	869	865	862	863
ν W=O	936	933	933	932	932
ν C–O	1007	1045	1032	1031	-
	1058		1072	1067	-
	1110	1113	1120	1118	-

2. Thermogravimetric analysis

Table S2. TGA data for compounds Na_3**CrW_6-(tris-C_2H_5)$_2$**·$13H_2O$, Na_2K_4**CrW_6-tris-C_2H_5**·$17H_2O$, Na_5**CrW_6-tris-NH_3**·$17H_2O$ and $Na_4(TMA)_2$**CrW_6-tris-CH_2OH**·$19H_2O$ (See Fig. S2 – S5).

Compound	Step	T, ºC	Mass-loss, %	Number of water and Tris-R molecules corresponding to mass-loss
Na_3**CrW_6-(tris-C_2H_5)$_2$**·$13H_2O$	I	25-200	4.46	5 H_2O
	II	200-320	4.01	4.5 H_2O
	III	320-375	2.16	2.5 H_2O
	IV	375-700	7.70	2 $(CH_2)_3CC_2H_5$
Na_5**CrW_6-tris-NH_3**·$17H_2O$	I	25-150	10.25	11.5 H_2O
	II	150-300	1.15	1.5 H_2O
	III	300-425	2.45	3 H_2O
	IV	425-480	0.74	1 H_2O
	V	480-600	0.85	1 $(CH_2)_3CNH_2$
$Na_4(TMA)_2$**CrW_6-tris-CH_2OH**·$19H_2O$	I	25-195	13.38	16 H_2O
	II	195-400	11.81	3 H_2O + 2 TMA
	III	400-600	3.20	1 $(CH_2)_3CCH_2OH$
Na_3K_3**CrW_6-tris-C_2H_5**·$17H_2O$	I	25-92	5.57	6.5 H_2O
	II	92-200	4.63	5.5 H_2O
	III	200-375	4.48	5 H_2O
	IV	375-600	3.81	1 $(CH_2)_3CC_2H_5$

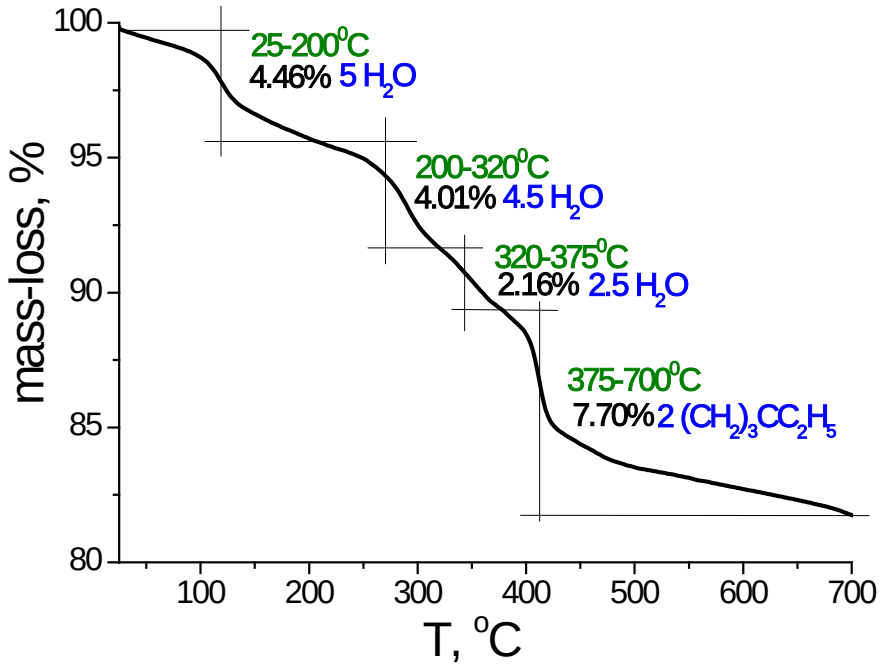

Figure S2. Thermogravimetric curve of Na_3**CrW_6-(tris-C_2H_5)$_2$**·$13H_2O$.

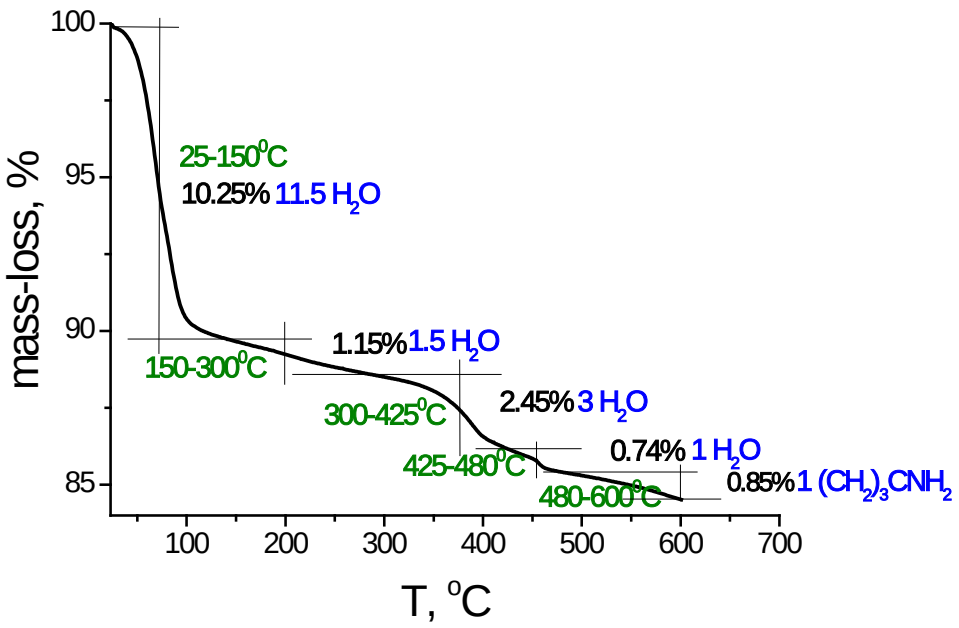

Figure S3. Thermogravimetric curve of Na_5**CrW_6-tris-NH_3**·**$17H_2O$.

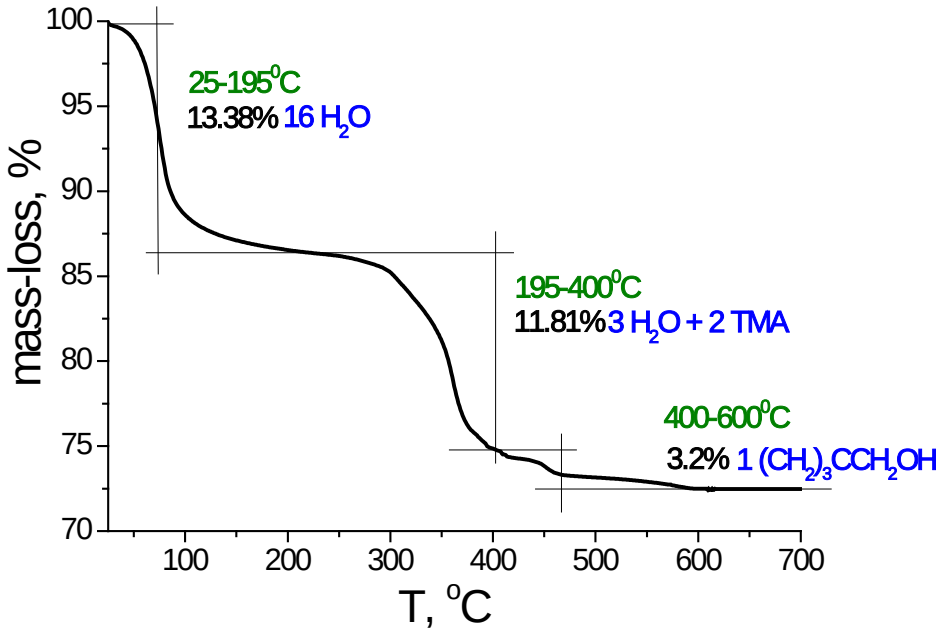

Figure S4. Thermogravimetric curve of $Na_4(TMA)_2$**CrW_6-tris-CH_2OH**·**$19H_2O$.

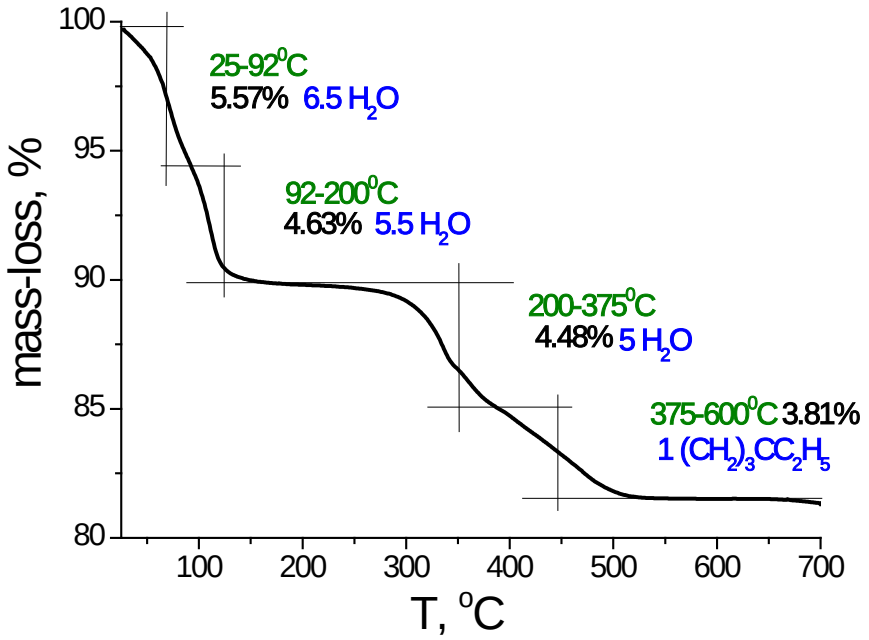

Figure S5. Thermogravimetric curve of Na_3K_3**CrW_6-tris-C_2H_5**$\cdot 17H_2O$.

3. ESI-MS

All compounds were investigated with an ESI-Qq-oaRTOF supplied by Bruker Daltonics Ltd. Bruker Daltonics Data Analysis software was used to analyze the results. The measurement was carried out in a 1:1 mixture of water/MeCN, collected in negative ion mode and with the spectrometer calibrated with the standard tune-mix to give an accuracy of *ca.* 5 ppm in the region of *m/z* 300-3000.

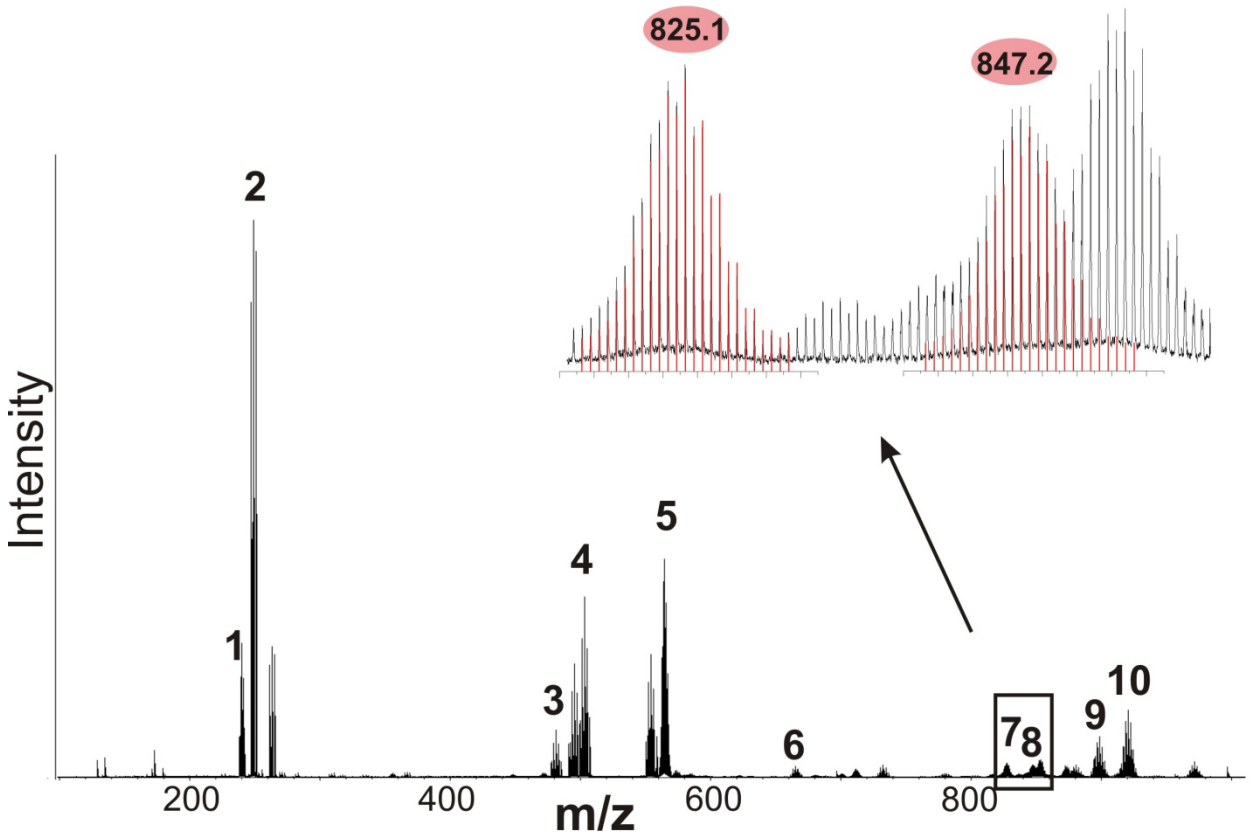

Figure S6. Negative ion-mode ESI-MS spectrum of **$Na_4(TMA)_2CrW_6$-tris-CH_2OH** in H_2O/CH_3CN. ESI-MS peak envelopes of $Na_xH_{4-x}[CrW_6O_{21}(OCH_2)_3CCH_2OH]^{2-}$ (x = 1, 3; experimental pattern, black; simulated pattern, red).

Table S3. Species assigned to the peaks in the ESI-MS spectrum of **$Na_4(TMA)_2CrW_6$-tris-CH_2OH** (see Fig. S6).

	m/z	m/z (calc.)	Peak Assignment
1	239.9	239.9	$[W_2O_7]^{2-}$
2	248.9	248.9	$H[WO_4]^-$
3	480.9	480.9	$H[W_2O_7]^-$
4	502.8	502.7	$Na[W_2O_7]^-$
5	564.4	564.4	$[CrW_4O_{13}(OCH_2)_3CCH_2OH]^{2-}$
6	680.2	680.2	$[CrW_5O_{16}(OCH_2)_3CCH_2OH]^{2-}$
7	**825.1**	**825.1**	**$NaH_3[CrW_6O_{21}(OCH_2)_3CCH_2OH]^{2-}$**
8	**847.2**	**847.1**	**$Na_3H[CrW_6O_{21}(OCH_2)_3CCH_2OH]^{2-}$**
9	897.8	897.8	$H[CrW_3O_{10}(OCH_2)_3CCH_2OH]^-$
10	919.8	919.6	$Na[CrW_3O_{10}(OCH_2)_3CCH_2OH]^-$

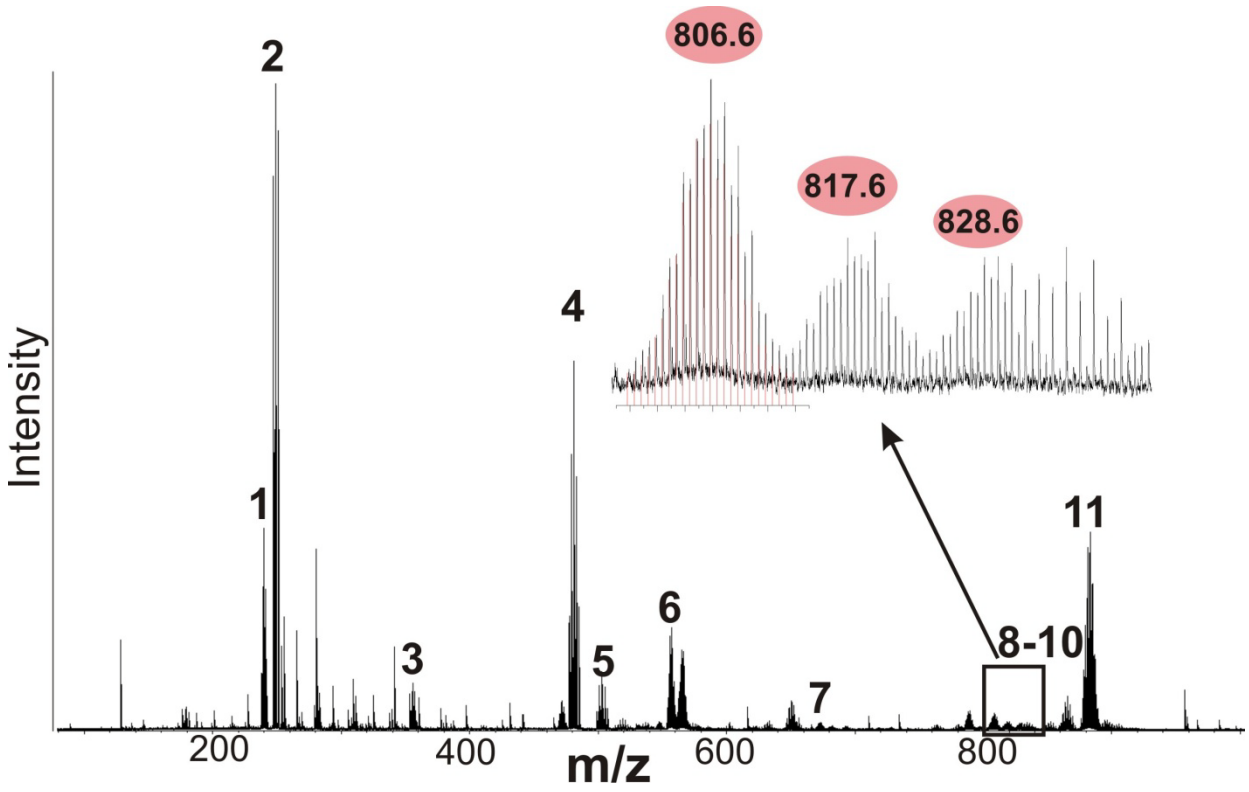

Figure S7. Negative ion-mode ESI-MS spectrum of Na_5**CrW_6-tris-NH_3** in mixed H_2O/CH_3CN. ESI-MS peak envelope of $H_4[CrW_6O_{21}(OCH_2)_3CNH_2]^{2-}$ (experimental pattern, black; simulated pattern, red).

Table S4. Species assigned to the peaks in the ESI-MS spectrum Na_5**CrW_6-tris-NH_3** (see Fig. S7).

	m/z	m/z (calc.)	Peak Assignment
1	239.9	239.9	$[W_2O_7]^{2-}$
2	248.9	248.9	$H[WO_4]^-$
3	355.9	355.9	$[W_3O_{10}]^{2-}$
4	480.9	480.9	$H[W_2O_7]^-$
5	502.8	502.7	$Na[W_2O_7]^-$
6	556.6	556.6	$[CrW_4O_{13}(OCH_2)_3CNH_2]^{2-}$
7	672.8	672.8	$[CrW_5O_{16}(OCH_2)_3CNH_2]^{2-}$
8	**806.6**	**806.6**	$\mathbf{H_3[CrW_6O_{21}(OCH_2)_3CNH_3]^{2-}}$
9	**817.6**	**817.6**	$\mathbf{NaH_2[CrW_6O_{21}(OCH_2)_3CNH_3]^{2-}}$
10	**828.6**	**828.6**	$\mathbf{Na_2H[CrW_6O_{21}(OCH_2)_3CNH_3]^{2-}}$
11	882.6	882.8	$[CrW_3O_{10}(OCH_2)_3CNH_3]^-$

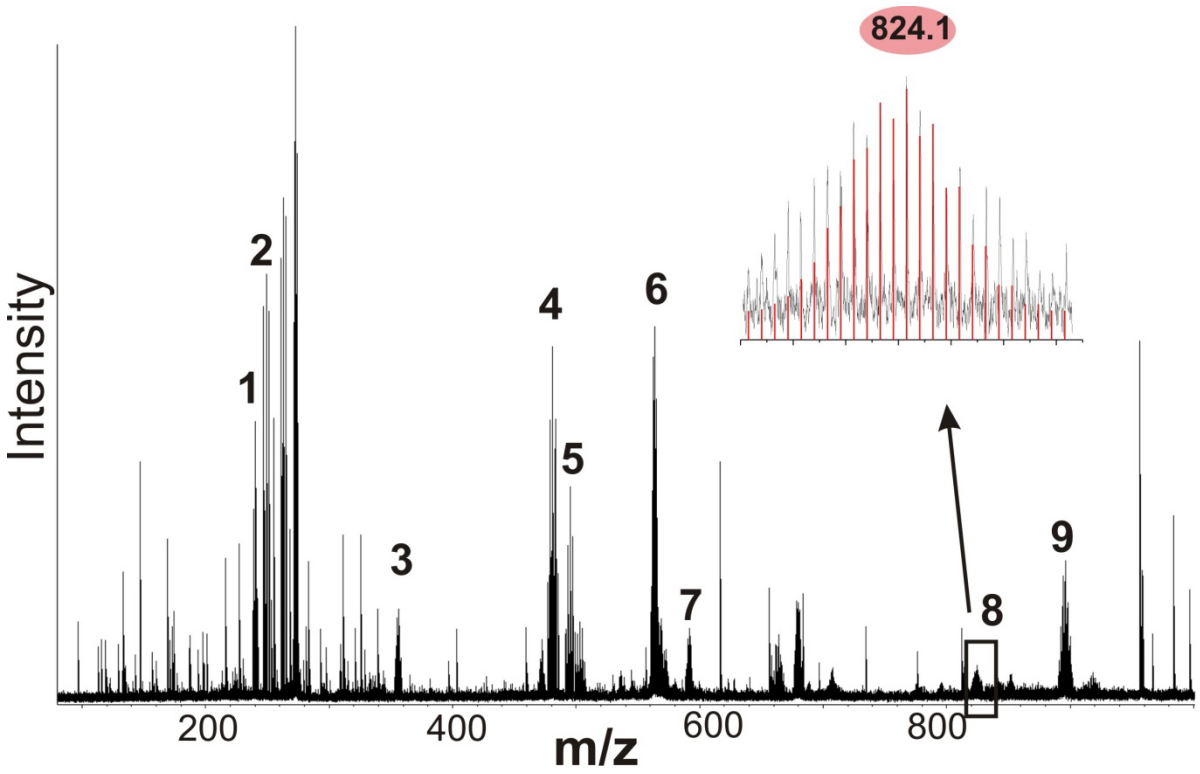

Figure S8. Negative ion-mode ESI-MS spectrum of Na_6**CrW_6-tris-C_2H_5** in mixed H_2O/CH_3CN. ESI-MS peak envelope of $NaH_3[CrW_6O_{21}(OCH_2)_3CC_2H_5]^{2-}$ (experimental pattern, black; simulated pattern, red).

Table S5. Species assigned to the peaks in the ESI-MS spectrum Na_6**CrW_6-tris-C_2H_5** (see Fig. S8).

	m/z	m/z (calc.)	Peak Assignment
1	239.9	239.9	$[W_2O_7]^{2-}$
2	248.9	248.9	$H[WO_4]^-$
3	355.9	355.9	$[W_3O_{10}]^{2-}$
4	480.9	480.9	$H[W_2O_7]^-$
5	502.8	502.7	$Na[W_2O_7]^-$
6	563.4	563.4	$[CrW_4O_{13}(OCH_2)_3CC_2H_5]^{2-}$
7	679.2	679.2	$[CrW_5O_{16}(OCH_2)_3CC_2H_5]^{2-}$
8	**824.1**	**824.1**	**$NaH_3[CrW_6O_{21}(OCH_2)_3CC_2H_5]^{2-}$**
9	895.7	895.7	$H[CrW_3O_{10}(OCH_2)_3CC_2H_5]^-$

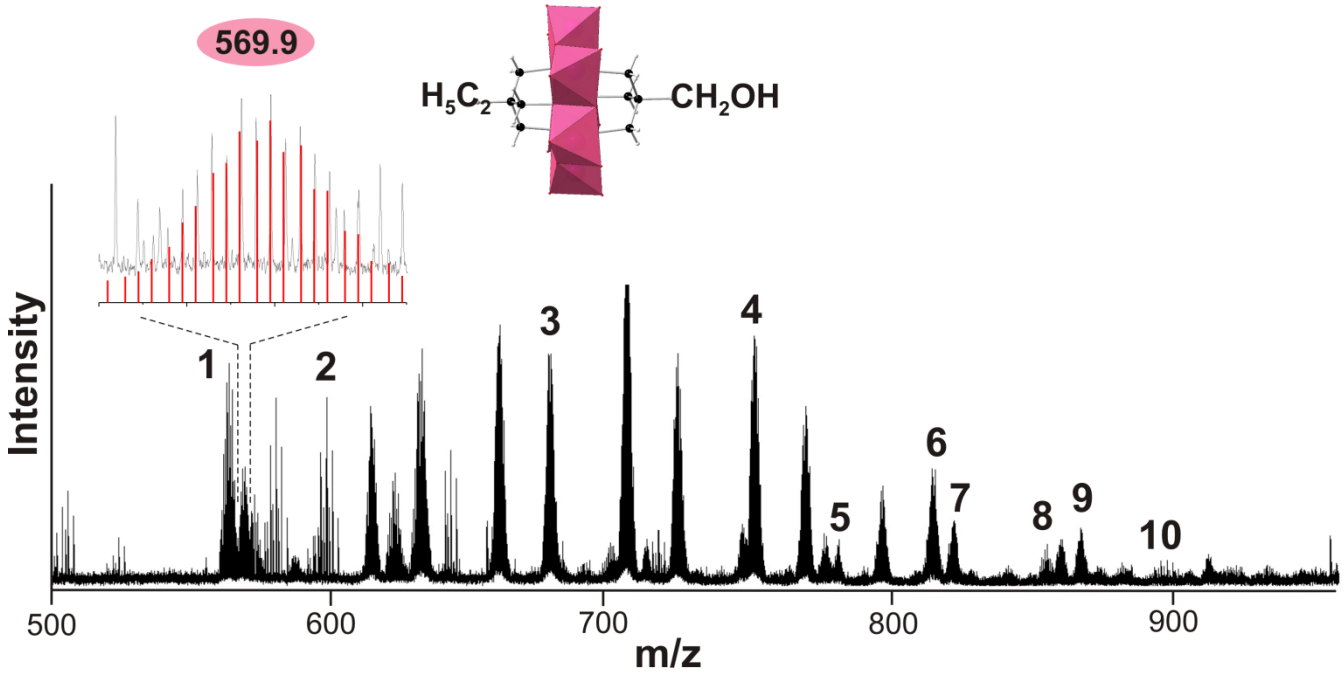

Figure S9. Negative ion-mode ESI-MS spectrum of the reaction mixture (30 mg of Na_6**CrW_6-tris-C_2H_5** with 50 mg of pentaerythritol (Tris-CH_2OH) were dissolved in 15 mL of H_2O and heated at 160 ºC for 48 hours) with CH_3CN. ESI-MS peak envelope of **$[CrW_6O_{18}(OCH_2)_6CCH_2OH(CC_2H_5)]^{3-}$** (experimental pattern, black; simulated pattern, red).

Table S6. Species assigned to the peaks in the ESI-MS spectrum of the reaction mixture after asymmetric functionalization (see Fig. S9).

	m/z	m/z (calc.)	Peak Assignment
1	564.4	564.4	$[CrW_4O_{13}(OCH_2)_3CCH_2OH]^{2-}$
	569.9	**569.9**	**$[CrW_6O_{18}(OCH_2)_6CCH_2OH(CC_2H_5)]^{3-}$**
2	605.8	605.8	$[CrW_4O_{10}(OCH_2)_6CCH_2OH(CC_2H_5)]^{2-}$
3	680.2	680.2	$[CrW_5O_{16}(OCH_2)_3CCH_2OH]^{2-}$
4	747.4	747.4	$H[CrW_5O_{16}(OCH_2)_6\ CCH_2OH(CC_2H_5)]^{2-}$
5	779.7	779.7	$[CrW_3O_{11}]^{-}$
6	813.3	813.3	$H_4[CrW_6O_{21}(OCH_2)_3CC_2H_5]^{2-}$
7	824.1	824.1	$NaH_3[CrW_6O_{21}(OCH_2)_3CC_2H_5]^{2-}$
8	855.3	855.3	$H[Cr((OCH_2)_3CCH_2OH)_2W_6O_{18}]^{2-}$
9	866.3	866.3	$Na[Cr((OCH_2)_3CCH_2OH)_2W_6O_{18}]^{2-}$
10	897.8	897.8	$H[CrW_3O_{10}(OCH_2)_3CCH_2OH]^{-}$

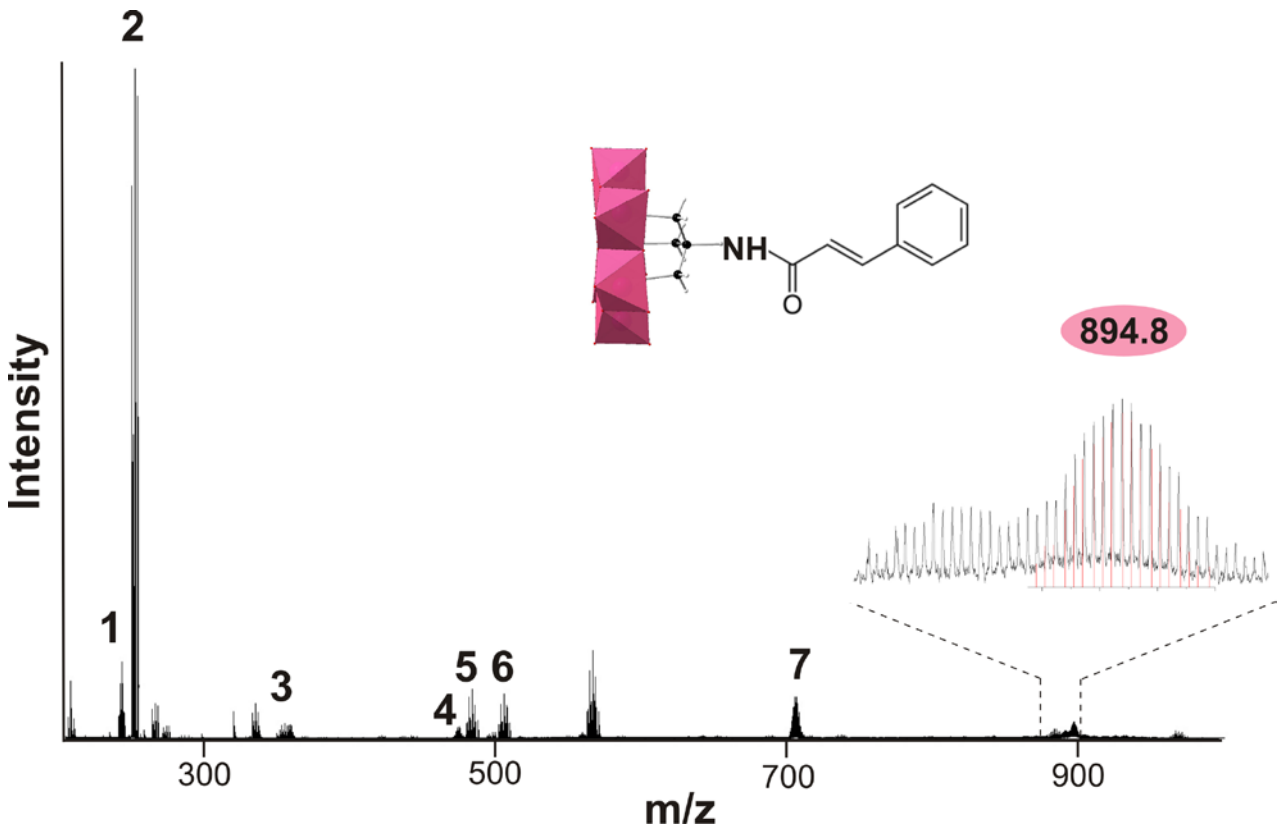

Figure S10. Negative ion-mode ESI-MS spectrum of the reaction mixture (300 mg of TBA_6**CrW_6-tris-NH_2** with 25 mg of cinnamic acid and 25 mg of EEDQ (N-ethoxycarbonyl-2-ethoxy-1,2-dihydroquinoline) were dissolved in 9.00 mL of CH_3CN and stirred at 50ºC for 24 h). ESI-MS peak envelope of **$Na_2H_2[CrW_6O_{21}(OCH_2)_3CNHC_9OH_7]^{2-}$** (experimental pattern, black; simulated pattern, red).

Table S7. Species assigned to the peaks in the ESI-MS spectrum of the reaction mixture after post-functionalization (see Fig. S10).

	m/z	m/z (calc.)	Peak Assignment
1	239.9	239.9	$[W_2O_7]^{2-}$
2	248.9	248.9	$H[WO_4]^-$
3	355.9	355.9	$[W_3O_{10}]^{2-}$
4	471.9	471.9	$[W_4O_{13}]^{2-}$
5	480.9	480.9	$H[W_2O_7]^-$
6	502.8	502.7	$Na[W_2O_7]^-$
7	703.8	703.8	$[W_6O_{19}]^{2-}$
	894.8	**894.8**	**$Na_2H_2[CrW_6O_{21}(OCH_2)_3CNHC_9OH_7]^{2-}$**

4. ESI-MS solution study

ESI-MS solution preparation. The stock solution of Cr^{3+} – WO_4^{2-} (C_w = 0.2 M) – H^+ was prepared at a molar ratio of 1:6:6 ($Cr:W:H^+$) and a final pH of 5.7 as described in the synthetic section of this SI. The 0.5 ml aliquots were taken after 1, 3 and 10 days after the solution preparation and the volume was adjusted to 10 ml with H_2O. Then 0.5 ml of these solutions was made up to 5 ml with H_2O/CH_3CN 1:1 mixture for direct injection into the ESI-MS system. The 2 parallel probes for the reaction mixture in the second day after solution preparation with pH of 5 and 7 were made using the diluted HCl and NaOH.

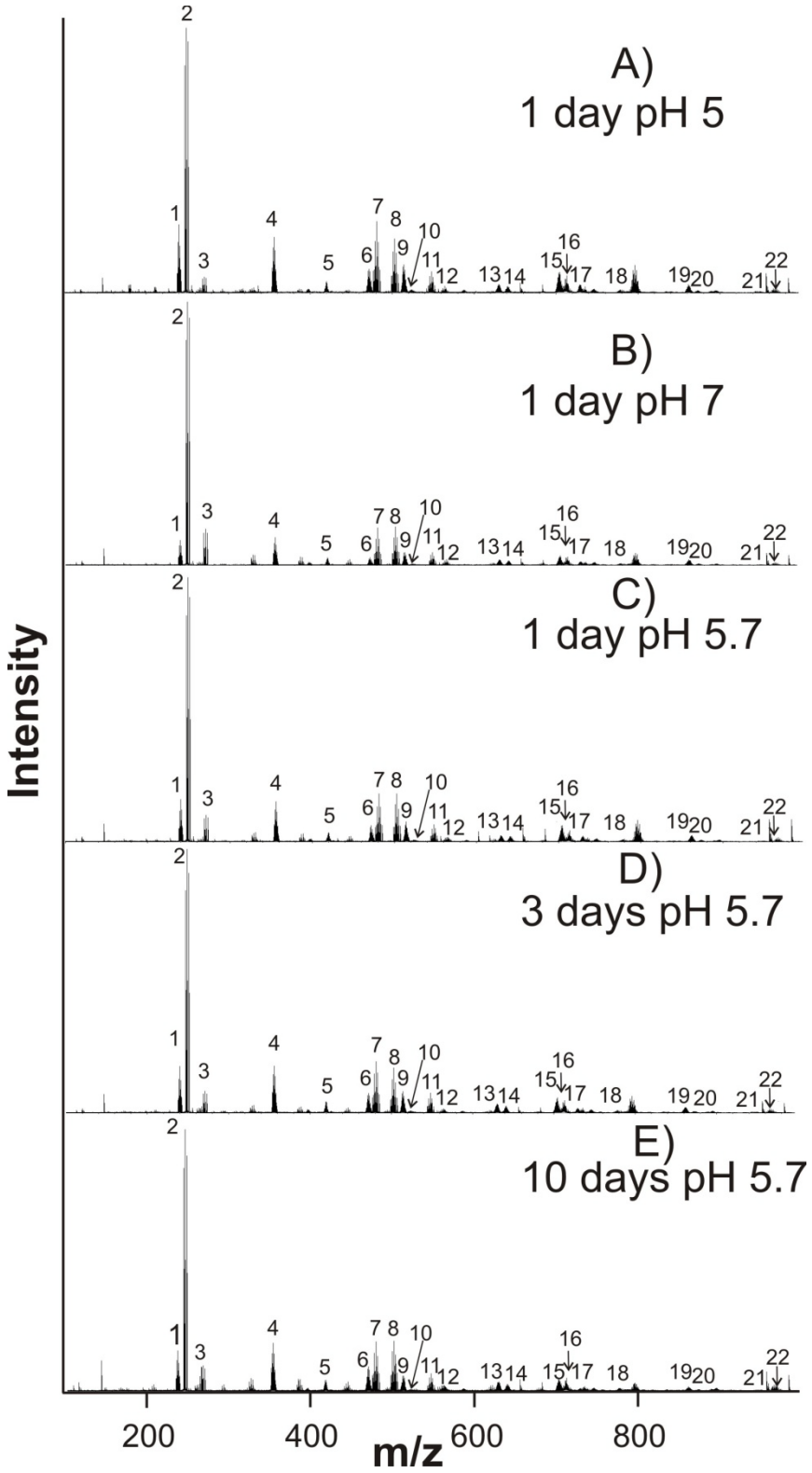

Table S8. Species assigned to the peaks in the ESI-MS spectra of the stock solutions Cr^{3+} – WO_4^{2-} – H^+ (see Fig. S11).

	m/z	m/z (calc.)	Peak assignment
1	239.9	239.9	$[W_2O_7]^{2-}$
2	248.9	248.9	$H[WO_4]^-$
3	270.9	270.9	$Na[WO_4]^-$
4	355.9	355.9	$[W_3O_{10}]^{2-}$
5	419.9	419.9	$[\mathbf{Cr}W_5O_{18}]^{3-}$
6	471.9	471.9	$[W_4O_{13}]^{2-}$
7	480.9	480.9	$H[W_2O_7]^-$
8	502.8	502.7	$Na[W_2O_7]^-$
9	514.3	514.3	$H[\mathbf{Cr}W_4O_{15}]^{2-}$
10	525.3	525.3	$Na[\mathbf{Cr}W_4O_{15}]^{2-}$
11	547.8	547.8	$[\mathbf{Cr}W_2O_8]^-$
12	587.8	587.8	$[W_5O_{16}]^{2-}$
13	630.3	630.3	$H[\mathbf{Cr}W_5O_{18}]^{2-}$
14	641.3	641.3	$Na[\mathbf{Cr}W_5O_{18}]^{2-}$
15	703.8	703.8	$[W_6O_{19}]^{2-}$
16	712.8	712.8	$H[W_3O_{10}]^-$
17	734.8	734.8	$Na[W_3O_{10}]^-$
18	779.7	779.7	$[\mathbf{Cr}W_3O_{11}]^-$
19	862.2	862.2	$H[\mathbf{Cr}W_7O_{24}]^{2-}$
20	873.2	873.2	$Na[\mathbf{Cr}W_7O_{24}]^{2-}$
21	944.7	944.7	$H[W_4O_{13}]^-$
22	966.7	966.7	$Na[W_4O_{13}]^-$

Figure S11. Negative ion-mode ESI-MS spectra of stock solutions Cr^{3+} – WO_4^{2-} – H^+ measured after 1, 3 and 10 days and at different pH (5.7; 5; 7) for the solution after 1 day of reaction. All spectra do not contain signals at *m/z* = 515.19, 773.29 or 784.27 assigned to $[Cr(OH)_6W_6O_{18}]^{3-}$, $H[Cr(OH)_6W_6O_{18}]^{2-}$ and $Na[Cr(OH)_6W_6O_{18}]^{2-}$, respectively.

For real-time observation of the self-assembly of **CrW_6-(tris-C_2H_5)$_2$** under hydrothermal condition the 0.5 ml aliquots of the reaction solution (prepared as described in the synthetic section of this SI) were taken after 12, 24 and 48 hours from the moment the reaction has been started.

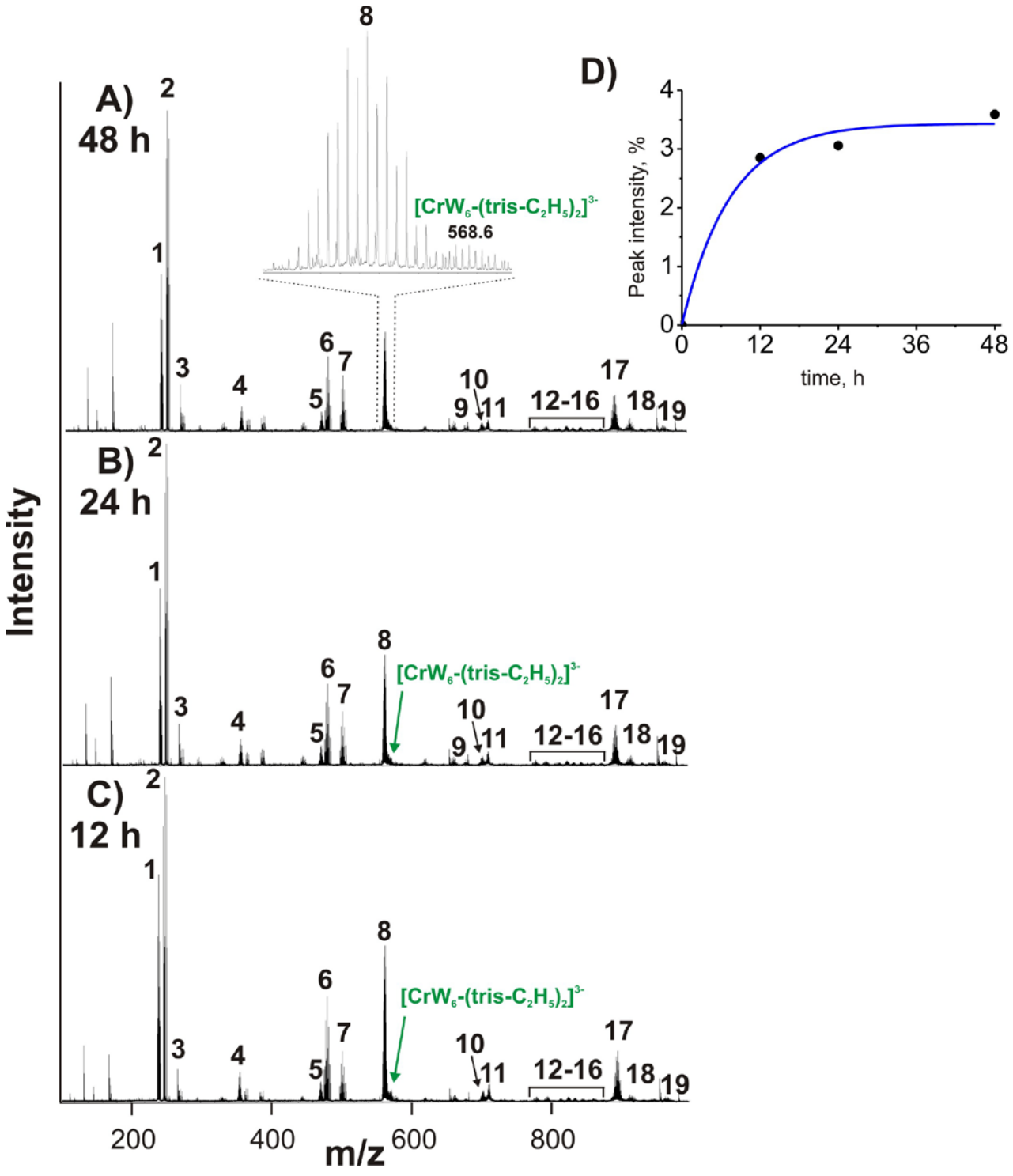

Figure S12. Negative ion-mode ESI-MS spectra of reaction (HT, 160 ºC) solutions Cr^{3+} – WO_4^{2-} – H^+ – Tris-C_2H_5 measured after 12 (C), 24 (B) and 48 (A) hours from the moment the reaction has been started. The assigned peaks (Table S8) were found in all spectra. All spectra do not contain signals at *m/z* = 515.19, 773.29 or 784.27 assigned to $[Cr(OH)_6W_6O_{18}]^{3-}$, $H[Cr(OH)_6W_6O_{18}]^{2-}$ and $Na[Cr(OH)_6W_6O_{18}]^{2-}$, respectively. Graphs (D) shows the general trend of increasing peak intensity of the target anion $[Cr((OCH_2)_3CC_2H_5)_2W_6O_{18}]^{3-}$.

Table S9. Species assigned to the peaks in the ESI-MS spectra of the reaction solution of Cr^{3+} – WO_4^{2-} – H^+ – Tris-C_2H_5 (see Fig. S12).

	m/z	m/z (calc.)	Peak Assignment
1	239.9	239.9	$[W_2O_7]^{2-}$
2	248.9	248.9	$H[WO_4]^-$
3	270.9	270.9	$Na[WO_4]^-$
4	355.9	355.9	$[W_3O_{10}]^{2-}$
5	471.9	471.9	$[W_4O_{13}]^{2-}$
6	480.9	480.9	$H[W_2O_7]^-$
7	502.8	502.7	$Na[W_2O_7]^-$
8	563.4	563.4	$[CrW_4O_{13}(OCH_2)_3CC_2H_5]^{2-}$
	568.6	**568.6**	$\mathbf{[Cr((OCH_2)_3CC_2H_5)_2W_6O_{18}]^{3-}}$
9	679.2	679.2	$[CrW_5O_{16}(OCH_2)_3CC_2H_5]^{2-}$
10	703.8	703.8	$[W_6O_{19}]^{2-}$
11	712.8	712.8	$H[W_3O_{10}]^-$
12	779.7	779.7	$[CrW_3O_{11}]^-$
13	**835.3**	**835.3**	$\mathbf{Na_2H_2[Cr(OCH_2)_3CC_2H_5W_6O_{21}]^{2-}}$
14	**845.8**	**845.8**	$\mathbf{Na_3H[Cr(OCH_2)_3CC_2H_5W_6O_{21}]^{2-}}$
15	**853.4**	**853.4**	$\mathbf{H[Cr((OCH_2)_3CC_2H_5)_2W_6O_{18}]^{2-}}$
16	**864.3**	**864.3**	$\mathbf{Na[Cr((OCH_2)_3CC_2H_5)_2W_6O_{18}]^{2-}}$
17	895.7	895.7	$H[CrW_3O_{10}(OCH_2)_3CC_2H_5]^-$
18	944.7	944.7	$H[W_4O_{13}]^-$
19	966.7	966.7	$Na[W_4O_{13}]^-$

5. Electrochemistry

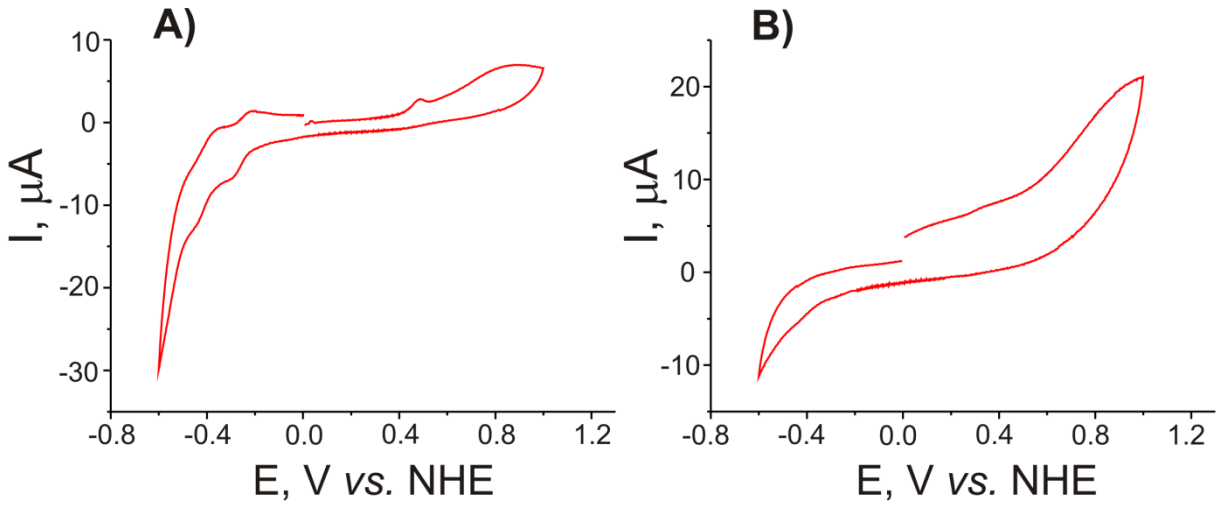

Figure S13. Cyclic voltammogram of 2mM solutions of **CrW_6-tris-C_2H_5** (A) and **CrW_6-(tris-C_2H_5)$_2$** (B) at scan rate of 0.100 $V \cdot s^{-1}$ at a glassy carbon electrode (d = 3 mm) vs. normal hydrogen electrode (NHE) in 1 M acetate buffer with pH 5.7.

6. X-ray Crystallography

The X-ray data were measured on a Bruker D8 Venture equipped with a multilayer monochromator, MoKα INCOATEC micro focus sealed tube and Kryoflex cooling device. The structure was solved by direct methods and refined by full-matrix least-squares. Non-hydrogen atoms were refined with anisotropic displacement parameters. Hydrogen atoms were inserted at calculated positions and refined with riding coordinates. The following software was used for the structure solving procedure: Frame integration, Bruker SAINT software package [1] using a narrow-frame algorithm (absorption correction), SADABS [2] (structure solution), SHELXS-2013 [3] (refinement), SHELXL-2013, [3] OLEX2, [4] SHELXLE [5] (molecular diagrams), OLEX2. [4] Experimental data and CCDC-codes can be found in Table **S10**.

$Na_6[Cr(OH)_3W_6O_{21}] \cdot 21.75H_2O$ originally synthesized and crystallized by Kortz et al. [6], was synthesized and crystallized by an alternative procedure: 30 mL of an aqueous solution containing $Na_2WO_4 \cdot 2H_2O$ (3.3 g, 10 mmol) was heated at approximately 80 °C, followed by the addition of 0.1 g of boric acid. The final pH of the solution was adjusted to 7 with diluted HCl (1 M). $CrCl_3 \cdot 6H_2O$ (0.54 g, 2 mmol) dissolved in 2 mL water was added dropwise. A light turbidity occurred and it was waited until the solution cleared again before adding the next drop. After the complete addition of the $CrCl_3 \cdot 6H_2O$ solution, the mixture remained turbid. The final pH of 8 was adjusted by addition of diluted NaOH (1 M). The solution was stirred and heated to approximately 80 °C for half an hour. Afterwards the solution was cooled down to room temperature, centrifuged to remove unreacted educts and transferred to crystallization beakers. After several weeks, green single crystals were obtained.[7]

Table S10. Crystallographic data.

	CrW_6-(tris-C_2H_5)$_2$	CrW_6-tris-C_2H_5	CrW_6-tris-NH_2	CrW_6-tris-CH_2OH	CrW_6
Empirical formula	$C_{12}H_{44}CrNa_3O_{37}W_6$	$C_6H_{20}CrK_3Na_3O_{31}W_6$ [+ solvent]	$C_4H_{28}CrNNa_5O_{41}W_6$	$C_{13}H_{65}CrN_2Na_4O_{44}W_6$	$CrH_{43.5}Na_6O_{45.75}W_6$
CCDC/CSD	**1842741**	**1842742**	**1842739**	**1842740**	**1870211**
Formula weight M_r	2004.56	1935.73	2016.32	2182.66	2068.89
Crystal system	monoclinic	monoclinic	triclinic	monoclinic	triclinic
Space group	*C2/c*	*C2/m*	*P1*	*Cc*	*P1*
T, K	100	100	200	100	200
a, b, c (Å)	27.9468(17), 11.8789(6), 13.1267(6)	22.7813(14), 13.0347(8), 18.2057(11)	11.7546(6), 15.9479(8), 22.9680(12)	23.0969(9), 12.9414(4), 17.2931(6)	11.642(2), 12.341(3), 16.526(3)
α, β, γ (°)	90, 101.792(3), 90	90, 112.130(2), 90	71.809(2), 83.295(2), 79.051(3)	90, 103.067(2), 90	68.37(3), 85.30(3), 71.06(3)
V (Å^3)	4265.8(4)	5007.9(5)	4008.3(4)	5035.2(3)	2085.6(9)
Z	4	8	4	8	2
D_{calc}, g/cm^3	3.124	2.568	3.294	2.878	3.294
μ, mm^{-1}	16.494	29.619	17.579	14.003	16.915
Abs. correct. type	multi-scan	multi-scan	multi-scan	multi-scan	multi-scan
Abs. correct. Tmin	0.008	0.135	0.104	0.02	0.015
Abs. correct. Tmax	0.039	0.324	0.493	0.018	0.050
F(000)	3652.0	3460.0	3640.0	4040.0	1887.0
Crystal size, mm	0.25 × 0.25 × 0.05	0.23 × 0.11 × 0.05	0.11 × 0.09 × 0.02		
Theta range for data collection	2.35 – 30.10	1.99 – 36.45	2.46 – 33.59	3.14 – 33.30	2.21 – 30.3078
Index ranges	–33 ≤ h ≤ 33 –14 ≤ k ≤ 14 –15 ≤ l ≤ 15	–28 ≤ h ≤ 28 –16 ≤ k ≤ 16 –22 ≤ l ≤ 22	–14 ≤ h ≤ 14 –19 ≤ k ≤ 19 –27 ≤ l ≤ 27	–27 ≤ h ≤ 27 –15 ≤ k ≤ 15 –20 ≤ l ≤ 20	–14 ≤ h ≤ 14 –14 ≤ k ≤ 14 –19 ≤ l ≤ 19
Reflections collected	42215	35802	87589	47755	43007
Rint	0.0411	0.0602	0.0331	0.0317	0.0358
Data / restraints / parameters	3875/21/287	5183/27/279	14657/122/1093	9159/110/711	7615/522/598
Goodness-of-fit on F^2	1.075	1.121	1.061	1.162	1.096
Final *R* indices	R_F = 0.0330, wR^2 = 0.1023 (all data) R_F = 0.0313, wR^2 = 0.1047 (I>2σ(I))	R_F = 0.0611, wR^2 = 0.1564 (all data) R_F = 0.0585, wR^2 = 0.1595 (I>2σ(I))	R_F = 0.03220, wR^2 = 0.0614 (all data) R_F = 0.02556, wR^2 = 0.0643 (I>2σ(I))	R_F = 0.0284, wR^2 = 0.0712 (all data) R_F = 0.0282, wR^2 = 0.0713 (I>2σ(I))	R_F = 0.0358, wR^2 = 0.0738 (all data) R_F = 0.0299, wR^2 = 0.0684 (I>2σ(I))
Largest diff. peak and hole, e. Å^{-3}	1.95/-1.94	0.42/-2.14	3.11/-1.43	0.60/-1.82	2.68/-2.30

7. Bond valence sum (BVS) calculation

BVS calculation [8,9] was applied to locate the protonation state of μ_3-O oxygen atoms in **CrW_6-tris-R** and in the parent $[Cr(OH)_3W_6O_{21}]^{6-}$ synthesized in this work (**Table S11**).

Table S11. Bond valence sum values for μ_3-O atoms in **CrW_6-tris-R** (R=-C_2H_5, -NH_2 -CH_2OH), which do not connect to the tris-ligand (blue in the figure), and for the six μ_3-O atoms in **$[Cr(OH)_3W_6O_{21}]^{6-}$**.

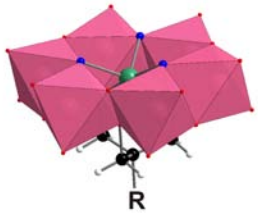

CrW_6-tris-C_2H_5 (CCDC 1842742)		**CrW_6-tris-NH_2** (CCDC 1842739)		**CrW_6-tris-CH_2OH** (CCDC 1842740)	
Atom	BVS values	Atom	BVS values	Atom	BVS values
O3	–1.73	O12	–1.73	O3	–1.69
O9	–1.65	O13	–1.72	O13	–1.68
		O15	–1.74	O22	–1.70

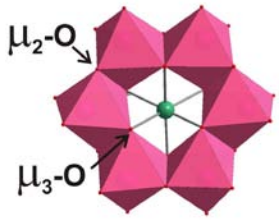

$[Cr(OH)_3W_6O_{21}]^{6-}$ (CSD 1870211)					
Atom	BVS values	Atom	BVS values	Atom	BVS values
O1	–1.73	O3	–1.71	O5	–1.72
O2	–1.18	O4	–1.22	O6	–1.11

8. DFT Calculations

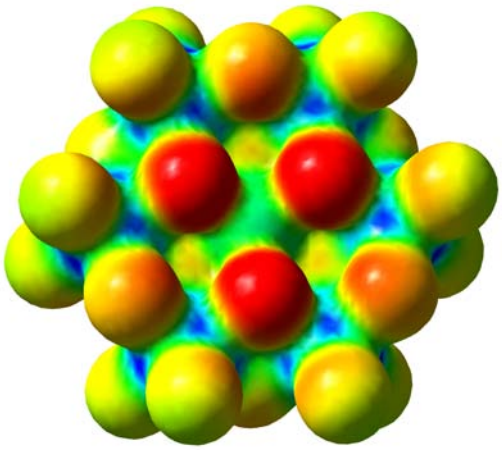

Figure S14. Molecular electrostatic potential for non-protonated CrW_6. Red identifies more nucleophilic regions and green denotes less nucleophilic regions. The colour vs. potential ranges from -1.089 (red) to -0.650 (blue).

Table S12. Relative enthalpies with respect to the monoprotonated **CrW_6** anion (proton on a triply-bridging oxygen (μ_3-O)), $[Cr(\mu_3\text{-}OH)_1W_6O_{23}]^{8-}$.

Anion	ΔH (kcal·mol^{-1})
$[Cr(\mu_3\text{-}OH)_1W_6O_{23}]^{8-}$	0
$[Cr(O_tH)_1W_6O_{23}]^{8-}$	+4.4
$[Cr(\mu_2\text{-}OH)_1W_6O_{23}]^{8-}$	+11.2

All structures were optimised and the vibrational modes were calculated with PBE0 exchange-correlation functional, the def2-TZVP basis set, and PCM as solvent model. $[Cr(O_tH)_1W_6O_{23}]^{8-}$ and $[Cr(\mu_2\text{-}OH)_1W_6O_{23}]^{8-}$ are the monoprotonated **CrW_6**, exhibiting the proton on a terminal oxygen (O_t) or doubly-bridging oxygen (μ_2-O) atom, respectively (see structures in the supplement xyz file).

Table S13. Relative enthalpies and relative enthalpies difference (in parenthesis) with respect to *fac*$_1$-$[Cr(OH)_3W_6O_{22}]^{6-}$ with different level of theory.

Anion	ΔH_{PBE0} (kcal·mol^{-1})	ΔH_{PBE} (ΔH_{PBE}-ΔH_{PBE0}) (kcal·mol^{-1})	ΔH_{B3LYP} (ΔH_{PBE}-ΔH_{PBE0}) (kcal·mol^{-1})
fac$_1$-$[Cr(OH)_3W_6O_{21}]^{6-}$	0	0	0
mer-$[Cr(OH)_3W_6O_{21}]^{6-}$	+3.7	+2.9 (+0.8)	+3.3 (+0.4)
fac$_2$-$[Cr(OH)_3W_6O_{21}]^{6-}$	+7.4	+6.6 (+0.8)	+7.7 (+0.3)

All structures were optimised and the vibrational modes were calculated with the indicated exchange-correlation functional, the def2-TZVP basis set, and PCM as solvent model.

Table S14. Spin angular momentum, enthalpy, entropy and Gibbs free energy for the different protonation states of $[Cr(OH)_xW_6O_{24-x}]^{(9-x)-}$ (x = 0 – 6).

Species	$S^{2,a}$	ε (a.u.)	H (a.u.)	S (cal/mol.K)	G (a.u.)
$[CrW_6O_{24}]^{9-}$	3.7730	-3253.84188071	-3253.724951	218.781	-3253.828901
$[Cr(\mu_3\text{-}OH)_1W_6O_{23}]^{8-b}$	3.7718	-3254.37144161	-3254.241943	217.040	-3254.345065
$[Cr(\mu_2\text{-}OH)_1W_6O_{23}]^{8-b}$	3.7742	-3254.35329294	-3254.224070	219.700	-3254.328457
$[Cr(O_tH)_1W_6O_{23}]^{8-b}$	3.7723	-3254.36408191	-3254.235001	217.989	-3254.338574
iso1-$[Cr(OH)_2W_6O_{22}]^{7-}$	3.7703	-3254.89078691	-3254.749180	221.059	-3254.854212
iso2-$[Cr(OH)_2W_6O_{22}]^{7-}$	3.7696	-3254.89074360	-3254.749020	220.503	-3254.853788
iso3-$[Cr(OH)_2W_6O_{22}]^{7-}$	3.7714	-3254.88522730	-3254.743162	218.743	-3254.847094
fac$_1$-$[Cr(OH)_3W_6O_{21}]^{6-}$	3.7685	-3255.40019215	-3255.246100	220.793	-3255.351006
mer-$[Cr(OH)_3W_6O_{21}]^{6-}$	3.7692	-3255.39438401	-3255.240089	223.137	-3255.346109
fac$_2$-$[Cr(OH)_3W_6O_{21}]^{6-}$	3.7707	-3255.38841724	-3255.234251	225.706	-3255.341491

iso1-$[Cr(OH)_4W_6O_{20}]^{5-}$	3.7682	-3255.88732093	-3255.720542	225.180	-3255.827532
iso2-$[Cr(OH)_4W_6O_{20}]^{5-}$	3.7694	-3255.88112230	-3255.714315	227.054	-3255.822196
iso3-$[Cr(OH)_4W_6O_{20}]^{5-}$	3.7680	-3255.88705351	-3255.720318	226.077	-3255.827734
iso4-$[Cr(OH)_4W_6O_{20}]^{5-}$	3.7694	-3255.88122944	-3255.714308	225.626	-3255.821510
$Cr(OH)_5W_6O_{19}]^{4-}$	3.7678	-3256.36282439	-3256.183209	227.963	-3256.291522
$Cr(OH)_6W_6O_{18}]^{3-}$	3.7672	-3256.82566019	-3256.632425	228.456	-3256.740972
H^{+}, [6]	-	-	-0.43805	-	-0.42068

Free energies are not symmetry corrected. [a]S^2 is the square of the total spin angular momentum. *Iso*$_n$ (n=1-4) refers to the different isomer of each protonation state using the same nomenclature as in the supplemental information. [b]μ_3-O, μ_2-O and O_t denote when the proton is localized on a triply-bridging oxygen (μ_3-O), doubly-bridging oxygen (μ_2-O) or terminal oxygen (O_t) atom, respectively. Structures of all isomers for each protonated state are provided in a separate multi-xyz file.

Table S15. Relative enthalpies with respect to the *iso1* (two protonated μ_3-O atoms from one side of the anion) isomer of $[Cr(OH)_2W_6O_{22}]^{7-}$ (see structures of isomers in the supplemental xyz file).

Anion	ΔH (kcal·mol^{-1})
iso1-$[Cr(OH)_2W_6O_{22}]^{7-}$	0
iso2-$[Cr(OH)_2W_6O_{22}]^{7-}$	+0.1
iso3-$[Cr(OH)_2W_6O_{22}]^{7-}$	+3.8

Table S16. Relative enthalpies with respect to the *iso1* (three protonated μ_3-O atoms on the same side and one protonated μ_3-O atom on the opposite side of the anion) isomer of $[Cr(OH)_4W_6O_{20}]^{5-}$ (see structures of isomers in the supplemental xyz file).

Anion	ΔH (kcal·mol^{-1})
iso1-$[Cr(OH)_4W_6O_{20}]^{5-}$	0
iso2-$[Cr(OH)_4W_6O_{20}]^{5-}$	+3.9
iso3-$[Cr(OH)_4W_6O_{20}]^{5-}$	+0.1
iso4-$[Cr(OH)_4W_6O_{20}]^{5-}$	+3.9

9. Powder X-ray diffraction

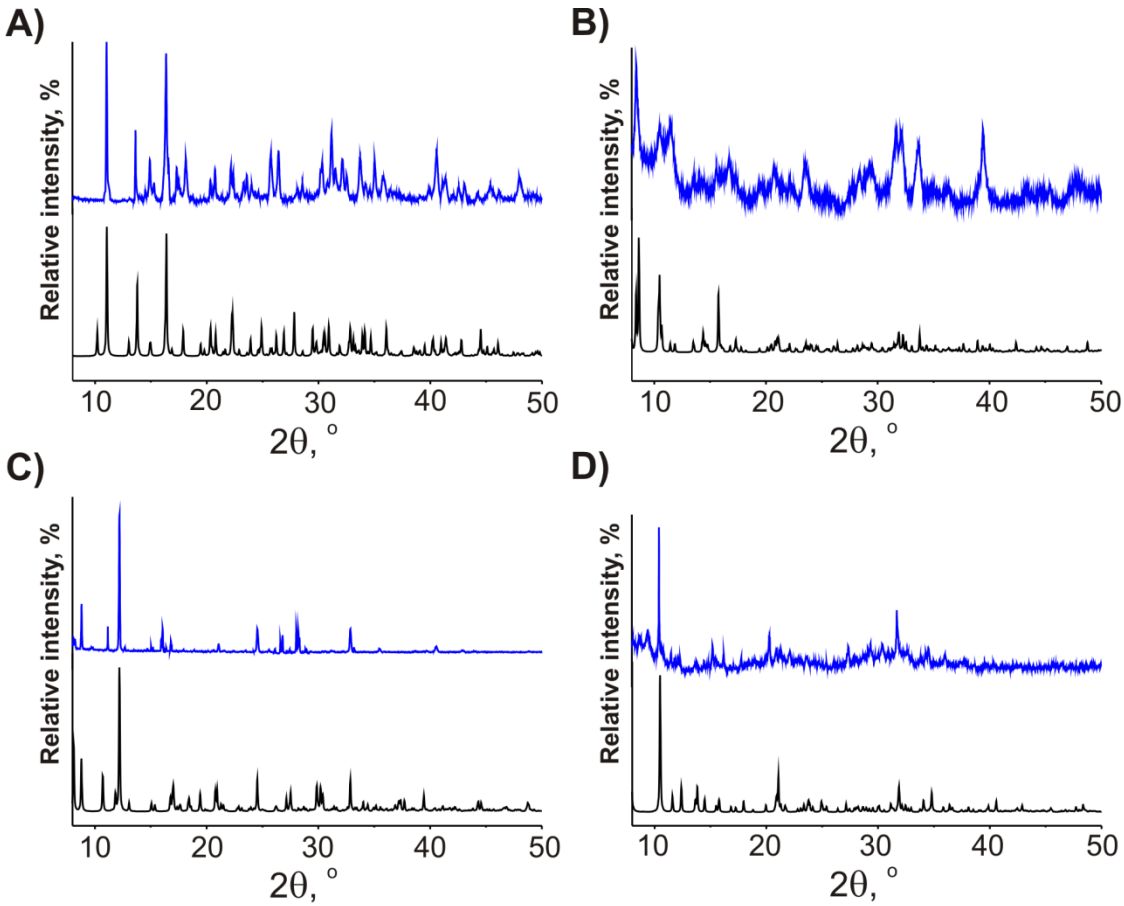

Figure S15. Experimental (blue) and simulated (black) X-ray diffraction patterns of A) Na_3CrW_6-(tris-C_2H_5)$_2$·$13H_2O$; B) $Na_3K_3CrW_6$-tris-C_2H_5·$17H_2O$; C) Na_5CrW_6-tris-NH_3·$17H_2O$; D) $Na_4(TMA)_2CrW_6$-tris-CH_2OH·$19H_2O$

References

1 Bruker SAINT V8.32B Copyright © 2005-2015 Bruker AXS.

2 Sheldrick, G. M. **1996**. *SADABS.* University of Göttingen, Germany.

3 Sheldrick, G. M. A short history of SHELX. *Acta Cryst. A,* **2008**, A64, 112-122.

4 Dolomanov, O. V.; Bourhis, L. J.; Gildea, R. J.; Howard, J. A. K.; Puschmann, H. OLEX2: a complete structure solution, refinement and analysis program. *J. Appl. Cryst.,* **2009**, *42*, 339-341.

5 Huebschle, C. B.; Sheldrick, G. M.; Dittrich, B. ShelXle: a Qt graphical user interface for SHELXL. *J. Appl. Cryst.*, **2011**, *44*, 1281-1284.

6 Liu, W.; Lin, Z.; Bassil, B. S.; Al-Oweini, R.; Kortz, U. Synthesis and Structure of Hexatungstochromate(III), $[H_3Cr^{III}W_6O_{24}]^{6-}$. CHIMIA, **2015**, *69*, 537-540.

7 Gumerova, N. I.; Roller, A.; Rompel, A. $[Ni(OH)_3W_6O_{18}(OCH_2)_3CCH_2OH]^{4-}$: the first tris-functionalized Anderson-type heteropolytungstate. *Chem. Commun.*, **2016**, 52, 9263-9266.

8 Brown, I. D.; Altermatt, D. Bond-valence parameters obtained from a systematic analysis of the Inorganic Crystal Structure Database. *Acta Cryst. B*, **1985**, *41*, 244-247.

9 Brese, N. E.; O'Keeffe, M. Bond-valence parameters for solids. *Acta Cryst. B*, **1991**, *47,* 192-197.